JOURNAL OF CATALYSIS **157**, 755–758 (1995)

NOTE

Potential Role of Penta-Coordinated Sulfur in the Acid Site Structure of Sulfated Zirconia

Two structures have been proposed for the sulfated zirconia acid site. Yamaguchi and co-workers have proposed a bidentate sulfate species containing a O=S=O moiety (1–4). Bensitel *et al.* have proposed a tridentate SO_4 species containing a single S=O moiety (5). We suggest that structures similar to those depicted in Fig. 1 are consistent with the known properties of sulfated zirconia and may be responsible for acid properties. In our proposed structures, each sulfur atom is surrounded by five different oxygens. The structure in Fig. 1a, which represents the Lewis acid form of the catalyst, can be conceptualized as arising from the insertion of a planar SO_3 molecule into the 001 crystallographic face of tetragonal ZrO_2. Indeed, sulfate metal oxides have been prepared by simply heating the oxide in the presence of SO_3 (6). Because of its strong Lewis acidity, the SO_3 sulfur would be expected to interact strongly with oxygen lone pairs on the oxide surface. The particularly favorable orientation depicted in Fig. 1 would also permit two of the SO_3 oxygens to coordinate with surface zirconium atoms, leaving a single S=O moiety oriented with the S=O bond perpendicular to the oxide surface. Water can attack the Lewis acidic zirconium atoms in the structure shown in Fig. 1a to produce the structure shown in Fig. 1b, which depicts a possible Brønsted acid form of the catalytic site. The proton associated with the sulfur-containing group in Fig. 1b would be easily accessible to species approaching the catalyst surface and weakly held by interactions with SO_3 and oxide oxygens.

The sulfated zirconia catalyst sample that was used in this study was prepared by a previously published procedure (7). Zirconium hydroxide (BET area 180 m^2/g) was precipitated from a 0.5 *M* zirconium tetrachloride solution by dropwise addition of NH_4OH. After heating in air at 473 K, sulfate was added by incipient wetness impregnation with a NH_4SO_4 solution, yielding a sulfate loading of 8 wt%. After drying, the catalyst was calcined in air at 873 K for 4 h. The surface area of the calcined sample was about 110 m^2/g. Thermogravimetry–mass spectrometry (TG–MS) and variable temperature diffuse reflectance infrared (VT-DRIFTS) measurements were made by using previously described apparatus and procedures (8).

High-temperature infrared measurements indicated that sulfated zirconia thermal decomposition involved the loss of sulfur containing species only. An S=O vibration absorbance band at 1393 cm^{-1} and overlapping S–O vibration bands at 1084, 1026, and 987 cm^{-1} diminished in intensity after the catalyst was heated above 673 K. Unlike the infrared spectral results reported by Yamaguchi and co-workers (1), no infrared absorbance band associated with sulfur containing species was detected at 1190 cm^{-1}. However, the S–O absorbance bands that diminished above 673 K can be correlated with similar absorbance bands reported by Bensitel *et al.* (5). Small differences between the frequencies of the S–O infrared bands that we detected and the corresponding bands reported by Bensitel *et al.* may have been the result of the temperature dependence of the S–O vibrations. The sulfated zirconia sample was maintained at 673 K for our infrared measurements whereas Bensitel *et al.* measured their spectra at room temperature (5).

Previously reported thermogravimetric studies of sulfated oxides indicate that the thermal decomposition of samples prepared by reacting oxides with SO_2 in excess O_2 yields the oxide with the same mass as was measured before the sulfur-containing groups were added to the oxide (9). By using TG–MS, we have determined that the primary products of sulfated zirconia thermal decomposition are SO_2 and O_2, which is consistent with previously reported mass spectrometric results (10). The facts that the absorbance band losses caused by heating sulfated zirconia correlate with spectral changes observed when sulfated zirconia is made by adsorption of SO_2 in excess O_2 and that SO_2 and O_2 are the main products of sulfated zirconia thermal decomposition suggest that the decomposition process may be the reverse of the formation reaction when SO_2 and O_2 are employed as reactants. After compensating for differences in the ionization cross-sectonal areas of SO_2 and O_2, TG–MS relative mass spectral ion intensities indicated that the amount of SO_2 formed during sulfated zirconia thermal decomposition exceeded the amount of O_2 formed by more than a factor of 2. A 2 : 1 $SO_2 : O_2$ ratio would suggest that thermal decomposition resulted in a stoichiometric loss of SO_3 (e.g., SO_2 and O) from sulfated zirconia samples, which would be expected for the thermal

0021-9517/95 $12.00

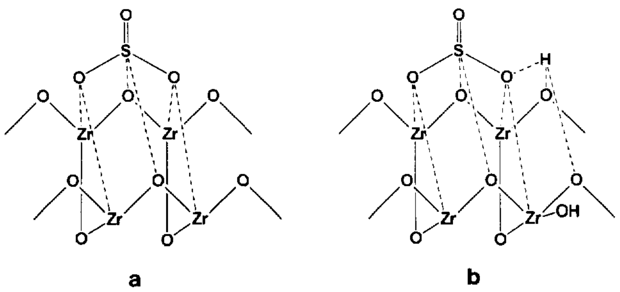

FIG. 1. Potential sulfated zirconia (a) Lewis and (b) Brønsted acid site structures.

decomposition of the structure shown in Fig. 1a. Interestingly, it has been shown that sulfated iron oxide can be prepared by heating the oxide in the presence of SO_3 whereas a similar thermal treatment in the presence of SO_2 without added O_2 does not result in the formation of acid sites (6). This finding supports the hypothesis that sulfation results in the addition of SO_3 to the oxide structure. The reason that the $SO_2:O_2$ ratio exceeded 2:1 was probably due to the fact that not all oxygen atoms formed by thermal decomposition of sulfated zirconia yielded O_2. Some oxygen atoms may have reacted with surface impurities to form small amounts of oxygenated organics instead of O_2.

Upon heating, zirconium hydroxide in contact with sulfur-containing species is converted into amorphous zirconium oxide that subsequently crystallizes into a tetragonal form, and, at higher temperature, this tetragonal form is converted to a monoclinic phase (10–13). The temperatures corresponding to the onset of crystallization and to the formation of the monoclinic phase are higher for sulfated zirconia than for zirconium oxide (4, 10–13). The temperature at which sulfate decomposition is detected for sulfated zirconia coincides with the ZrO_2 tetragonal to monoclinic phase transition (12), suggesting that monoclinic sulfated zirconia may not be stable.

In the tetragonal phase bulk, each zirconium atom is coordinated to eight different oxygens (14). Four Zr–O bonds are significantly shorter than the other four. The four short Zr-O bonds constitute one distorted tetrahedron and the four long Zr–O bonds constitute another distorted tetrahedron (14). In the absence of adsorbates, zirconium atoms at the 001 surface of tetragonal zirconium oxide are coordinated to only six different oxygens. Each zirconium atom can therefore interact with surface adsorbates through the two vacant coordination sites (15). We postulate that these surface coordination sites can be occupied by oxygenated sulfur species of the type shown in Fig. 1. The facts that crystallization can be retarded for sulfated zirconia and that the tetragonal phase is stabilized when sulfur-containing species is present indicate that the acid site structure is sensitive to the separation between the metal and oxygen atoms at the oxide surface. The multiple interactions depicted in Fig. 1 may not be possible for monoclinic ZrO_2 because the Zr–O–Zr spacing is too large.

Various Lewis bases interact with sulfated oxides causing shifts in the S=O stretching vibration frequency and the appearance of additional infrared bands that can be attributed to the adsorbed bases. CO adsorption on sulfated zirconia reveals that sulfation increases the oxide Lewis acidity relative to zirconium oxide (16, 17). However, infrared spectroscopic studies of H_2 and CH_4 adsorption, which probe Lewis acid–base pair polarizations, reveal that zirconia sulfation reduces its Lewis basicity (17). The strong interactions between the sulfur atom and Zr–O oxygens in our proposed structure (Fig. 1) would be expected to significantly reduce the Lewis basicity of the oxide oxygens while increasing the Lewis acidity of the zirconium atoms bonded to these oxygens via an inductive effect. Conversely, the coordination of these Lewis acid zirconium atoms by S–O oxygens would reduce the Lewis acidity of the zirconium atoms. The observed increase in Lewis acidity for sulfated zirconia (16, 17) may occur because the magnitude of the Lewis acidity reduction is less than the Lewis acidity enhancement. Pinna *et al.* have shown that sulfated zirconia catalytic activity for butane isomerization can be reversibly quenched by adsorption of CO on Lewis acid sites (18). These Lewis acid sites may be the nonhydroxylated zirconium atoms depicted in Fig. 1b. As shown in Fig. 1b, these zirconium atoms interact with SO_3 oxygens in the proposed Brønsted form of the acid site. It would be expected that adsorption of CO at these sites would affect Brønsted acidity and thus catalytic activity.

Infrared spectroscopy of adsorbed ammonia can be used to distinguish between Lewis and Brønsed acid sites (19). By measuring infrared spectra while heating samples containing adsorbed ammonia, spectral features corresponding to Brønsted (1450 cm^{-1}) and Lewis (1610 and 1250 cm^{-1}) acid sites were distinguished. After exposure to water, the sulfated zirconia sample examined in this study contained Brønsted acid sites, as evidenced by the appearance of an infrared band at 1450 cm^{-1} after ammonia adsorption. The partial removal of adsorbed ammonia by heating the sample from 373 to 473 K resulted in the infrared spectral changes shown in the difference spectrum in Fig. 2. The highest temperature to which the sample was exposed (473 K) was insufficient to decompose the sulfur-containing species. Therefore, the spectral features revealed in the difference spectrum in Fig. 2 were assigned to adsorbed ammonia and to changes in the environment of sulfur-containing species that resulted from ammonia desorption. The partial thermal desorption of ammonia caused an O–H stretching vibration at 3690 cm^{-1} to shift

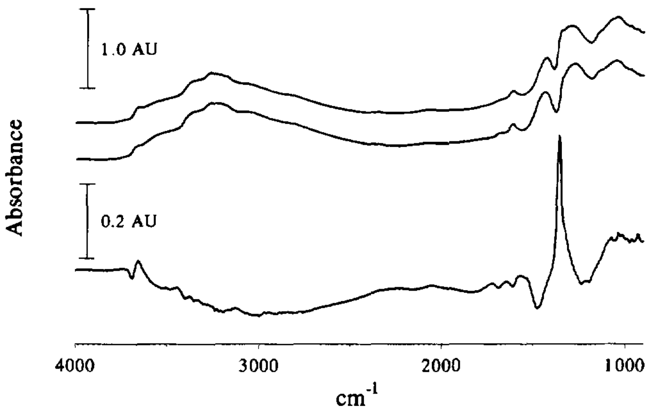

FIG. 2. Diffuse reflectance infrared spectra of sulfated zirconia containing adsorbed ammonia at 373 K (top) and 473 K (middle). The bottom difference spectrum is the result of subtracting the two absorbance spectra.

to 3660 cm^{-1}, a broadband loss of absorbance due to N–H stretching vibrations near 3000 cm^{-1}, the loss of absorbance at 1610 cm^{-1} due to NH_3 that desorbed from Lewis acid sites, the loss of absorbance at 1470 cm^{-1} due to NH_3 that desorbed from Brønsted acid sites, the appearance of a band near 1360 cm^{-1}, and a broadband loss of absorbance near 1200 cm^{-1}. Because the positive S=O (~1380 cm^{-1}) and the negative NH_4^+ (~1450 cm^{-1}) spectral features overlap in the difference spectrum, the band center intensities and peak frequencies corresponding to these species are not accurately represented by the absorbance maximum at 1360 cm^{-1} and the absorbance minimum at 1470 cm^{-1} in the difference spectrum. The broad negative spectral feature near 1200 cm^{-1} arises from the desorption of ammonia from Lewis acid sites and a reduction in the number of S=O groups interacting with ammonia. The positive absorbance band at 1360 cm^{-1} represents S=O groups that were released from interactions with ammonia by heating the sample.

The fact that the O–H band was present in infrared spectra before and after partial ammonia desorption suggests that the acidity of this hydroxyl was not sufficient to protonate ammonia at 373 K. The fact that the O–H stretching vibration band shifted to a lower frequency when ammonia was desorbed indicated that the O–H stretching vibraton force constant was greater when ammonia was present. This is the opposite of what would be expected for acidic O–H protons interacting with ammonia. Based on these observations, it seems likely that the O–H band shift shown in the difference spectrum in Fig. 2 resulted from a change in the environment of ZrO–H moieties that were not responsible for Brønsted acidity. In the structure shown in Fig. 1b, which can be obtained from the Fig. 1a structure by the attack of water on a zirconium atom Lewis acid site, the proton associated with the S–O oxygen would more likely be responsible for Brønsted acidity than the ZrOH proton. Because this proton would be loosely held and because many different environments would be possible for it, the O–H stretching vibration band for this proton would be expected to be broad and difficult to detect by infrared spectroscopy. On the basis of these arguments, the sharp 3658 cm^{-1} O–H stretching vibration band evident in the Fig. 2 difference spectrum can be assigned to Zr–O–H and the broad tail extending to lower frequencies could represent either hydrogen bonded Zr–O–H or S–O–H species.

Like sulfated zirconia, the infrared spectrum of thionyl tetrafluoride (SF_4O) contains a strong absorbance band near 1380 cm^{-1} that is assigned to the S=O stretching vibration (20, 21). Sulfur has five bonds and exists in the +6 oxidation state in thionyl tetrafluride. The structure of this molecule might be expected to have features in common with the proposed sulfated zirconia acid site shown in Fig. 1, in which sulfur is also in the +6 oxidation state and surrounded by five neighbors. The SF_4O molecule is trigonal bipyramidal, has C_{2v} symmetry, and the S=O moiety is located at the equatorial position (20). Two of the O=S–F bond angles are 90° and the other two O=S–F bond angles are 120° (21). The acid site structure shown in Fig. 1 can be considered a modification of the SF_4O structure in which oxygen atoms replace fluorines and the two 90° bond angles are increased due to interactions with zirconium atoms.

ACKNOWLEDGMENT

This work was supported by the National Science Foundation (CTS-9403199).

REFERENCES

1. Jin, T., Yamaguchi, T., and Tanabe, K., *J. Phys. Chem.* **90,** 4794 (1986).
2. Yamaguchi, T., Jin, T., Ishida, T., and Tanabe, T., *Mater. Chem. Phys.* **17,** 3 (1987).
3. Yamaguchi, T., *Appl. Catal.* **61,** 1 (1990).
4. Tanabe, K., Hattori, H., and Yamaguchi, T., *Crit. Rev. Surf. Chem.* **1,** 1 (1990).
5. Bensitel, M., Saur, O., Lavalley, J. C., and Morrow, B. A., *Mater. Chem. Phys.* **19,** 147 (1988).
6. Yamaguchi, T., Jin, T., and Tanabe, K., *J. Phys. Chem.* **90,** 3148 (1986).
7. Jatia, A., Chang, C., MacLeod, J. D., Okube, T., and Davis, M. E., *Catal. Lett.* **25,** 21 (1994).
8. Ai, J., Phegley, L. L., Christen, G., and White, R. L., *J. Am. Ceram. Soc.* **78,** 874 (1995).
9. Saur, O., Bensitel, M., Mohammed Saad, A. B., Lavalley, J. C., Tripp, C. P., and Morrow, B. A., *J. Catal.* **99,** 104 (1986).
10. Chokkaram, S., Srinivasan, R., Milburn, D. R., and Davis, B. H., *J. Colloid Interface Sci.* **165,** 160 (1994).

11. Chen, F. R., Coudurier, G., Joly, J. F., and Vedrine, J. C., *J. Catal.* **143,** 616 (1993).
12. Ward, D. A. and Ko, E. I., *J. Catal.* **150,** 18 (1994).
13. Sohn, J. R. and Kim, H. W., *J. Mol. Catal.* **52,** 361 (1989).
14. Teufer, G., *Acta Crystallogr.* **15,** 1187 (1962).
15. Babou, F., Bigot, B., and Sautet, P., *J. Phys. Chem.* **97,** 11501 (1993).
16. Morterra, C., Cerrato, G., Emanuel, C., and Bolis, V., *J. Catal.* **142,** 349 (1993).
17. Kustov, L. M., Kazansky, V. B., Figueras, F., and Tichit, D., *J. Catal.* **150,** 143 (1994).
18. Pinna, F., Signoretto, M., Strukul, G., Cerrato, G., and Morterra, C., *Catal. Lett.* **26,** 339 (1994).
19. Knozinger, H., *Adv. Catal.* **25,** 184 (1976).
20. Goggin, P. L., Roberts, H. L., and Woodward, L. A., *Trans. Faraday Soc.* **57,** 1877 (1961).
21. Radhakrishnan, M., *J. Mol. Spectrosc.* **10,** 111 (1963).

Robert L. White*[,1]
Emmanuel C. Sikabwe*
Mario A. Coelho†
Daniel E. Resasco†

**Department of Chemistry and Biochemistry*
†School of Chemical Engineering and Materials Science
University of Oklahoma
Norman, Oklahoma 73019

Received February 28, 1995; revised August 22, 1995; accepted August 29, 1995

---

[1] To whom correspondence should be addressed.